

## Degradation of imidacloprid in aqueous solutions by zero valent iron nanoparticles in the nitrogen medium

Cihan Gecgel<sup>a</sup>, Utku Bulut Simsek<sup>a</sup>, Meral Turabik<sup>a,b,\*</sup>

<sup>a</sup>Department of Nanotechnology and Advanced Materials, Mersin University, Mersin TR-33343, Turkey, Tel. +90 324 361 00 01; emails: mturabik@mersin.edu.tr (M. Turabik), cihangecgel@hotmail.com (C. Gecgel), utkubulutsimsek@msn.com (U.B. Simsek)

<sup>b</sup>Chemical Program, Technical Science Vocational School, Mersin University, Mersin TR-33343, Turkey

Received 17 July 2017; Accepted 7 April 2018

---

### ABSTRACT

Degradation of a neonicotinoid pesticide, imidacloprid (IMC), by zero valent iron nanoparticles (nZVI) was investigated in a batch manner as a function of nitrogen/air reaction medium, nZVI dosage, temperature and pH. The synthesis of nZVI was carried out by the reduction of ferric ions with borohydride method and characterized by scanning electron microscopy, energy dispersive X-ray, fourier transform infrared spectroscopy (FTIR), dynamic light scattering and X-ray diffractogram measurements. The results showed that the IMC removal efficiency was higher in nitrogen medium than in air medium. Also, pH and temperature strongly affected the degradation rates and increased nZVI amount enhanced the degradation efficiency of IMC. The decays of IMC with time well fitted to first-order reaction kinetics, also activation energy value of degradation process was determined as 54.68 kJ/mol. Three main compounds, IMC nitrosamine, IMC urea ketone and IMC keto urea, were determined by LC-ESI-MS/MS analysis as the degradation products and also a possible degradation mechanism was proposed. The chemical oxygen demand and inorganic ions measurements also showed low mineralization of IMC by using nZVI. The reusability studies and released ferrous and ferric ions measurement showed the long life of nZVI in nitrogen medium.

*Keywords:* Imidacloprid; Zero valent iron; Nanoparticle; Degradation; Nitrogen medium

---

### 1. Introduction

Pesticides have a wide production and application area in all over the world. With the rise of the world population, the production of agricultural products is also needed to increase and that can be achieved by the use of pesticides [1]. The United Nations estimate that all pesticides used in agriculture are only less than 1% of pesticides actually reaching the crops. The remaining pesticides contaminate the land, air and especially water [2]. Even a small amount of pesticides can show highly adverse effects to the environment such as toxicity to nontarget organisms, contamination of earth and groundwaters thus, their removal is imperative [1–3].

There are several groups and different chemical structures of pesticides. One of them is neonicotinoids that have been used for protecting crops from insect pests. Due to their superior physicochemical properties and high efficiencies to target insects, neonicotinoids have become the most extensively used class of pesticides in recent years. Today, they possess at least a quarter of the world pesticide market [4,5]. Neonicotinoids contain two main compounds which are nitro-substituted compounds (imidacloprid (IMC), clothianidin, dinotefuran, nitenpyram, thiamethoxam) and cyano-substituted compounds (thiacloprid and acetamiprid) [5]. IMC is commonly used as systematic pesticides for controlling many species such as termites and sucking insects. It is highly soluble in water (0.58 g/L) and also remains stable in it for more than 30 d [6]. Due to a higher lethal effect on the insects, IMC is the bestselling and most preferred neonicotinoid insecticides in the world,

---

\* Corresponding author.

but it can have a harmful effect on the nontarget insects and threaten human life [7,8]. But, a few effective technical solutions are available to remove the remaining IMC from within the environment.

Several physical, chemical as well as biological methods involving adsorption, oxidation, catalytic degradation, membrane filtration and biological treatments have been developed for the removal of pesticides [9]. But, still more efforts are needed to explore cost-effective methods. There are only a few studies made on the degradation of pesticides using nanoparticles. For this purpose, the most commonly used metallic nanoparticles are iron nanoparticles due to their high reactivity, low cost, easy production and nontoxicity [10].

Due to their significant surface area to weight ratio leading to a greater density of reactive sites, iron nanoparticles are particularly attractive for remediation purposes [11]. Therefore, zero valent iron (ZVI) has been extensively used as removal applications in water, soil and groundwater for heavy metals [11–13] pesticides [14–16], organic dyes [17–19], antibiotics [20,21], inorganic anions [21,22] and halogenated organic compounds [24,25] and also used as Fenton-like catalyst [20]/photocatalyst [26] for organic pollutants and a reactive material in permeable reactive barriers [23,27]. However, by the corrosion, various kinds of oxide, hydroxide, ferrous and/or ferric compounds may form on the surface of the ZVI. The resulting oxide forms on the surface of the particles may generally prevent the adsorption of contaminants or inhibit the surface reactions [15]. Thus, it is important to understand the effects of factors affecting surface corrosion, reactivity or reaction kinetics and to identify reaction intermediates and products.

There is no work about the degradation of IMC by using nanoparticles in an inert medium to protect the zero valent iron nanoparticles (nZVI) surface against the corrosion. In this study, to prevent the oxidation of the iron particles that cause the passivation of nanoparticles, an inert reaction medium was provided by feeding nitrogen gases to reaction medium for the degradation of IMC and compared with air reaction medium.

## 2. Materials and methods

### 2.1. Materials

IMC ( $C_9H_{10}ClN_5O_2$ ) was supplied from Sigma-Aldrich, Dresden, Germany with 99.9% purity. Its chemical structure and various properties are given in Table 1.

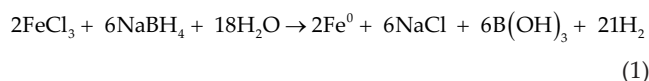
The chemicals used for the synthesis of nZVI and  $Fe_3O_4$  (magnetite) were obtained in high purity and used as received, including  $FeCl_3 \cdot 6H_2O$  (Merck KGaA, Darmstadt, Germany),  $FeSO_4 \cdot 7H_2O$  (Merck),  $NaBH_4$  (Merck),  $C_2H_5OH$  (Merck) and hexadecyltrimethylammonium bromide (HTAB, Sigma).

Acetonitrile ( $CH_3CN$ ) and formic acid (FA) used for the preparation of mobile phase in high pressure liquid chromatography (HPLC) and liquid chromatography electrospray ionization tandem mass spectrometry (LC/ESI-MS/MS) were obtained from Sigma-Aldrich. Sodium carbonate and methanesulphonic acid (MSA) employed in ion chromatography (IC) were analytical grade and obtained from Fluka and Acros Organics. Mix anion (Dionex Seven Anion Standard-II) and mix cation (Dionex Six Cation Standard-II) standards were

obtained from the Thermo Fisher Scientific, Waltham, MA, USA. The water used for the preparation of the solutions and analysis was obtained from a Millipore Milli-Q (simplicity 185) system with resistivity of  $>18$  M $\Omega$  cm.

### 2.2. Synthesis of ZVI and magnetite particles

The synthesis of nZVI was carried out in a three-neck flask by the reduction of ferric ions with the borohydride method in an inert atmosphere by using nitrogen gases to ensure anoxic conditions. HTAB was also used to stabilize the formed nZVI particles as described in the previous study [28]. Sodium borohydride was added dropwise to the solution in slight excess of the stoichiometric requirements for the reduction of  $Fe^{3+}$  to  $Fe^0$  (nZVI). The nZVI particles were synthesized according to the following reaction:



The obtained iron nanoparticles were washed three times with absolute ethanol, dried at 65°C for 4 h in a vacuum oven and stored in a vacuum medium for analysis.

ZVI may oxidize to iron oxides, especially to magnetite ( $Fe_3O_4$ ), in the presence of the oxygen. Generally, the formed magnetite on the surface of the nZVI causes the adsorption of the various compounds. The treatment of IMC by nZVI may result in either its degradation or surface adsorption. To investigate whether the adsorption of IMC by magnetite occurred or not, magnetite nanoparticles were synthesized through the coprecipitation method by adding a base to an aqueous mixture of  $Fe^{3+}$  and  $Fe^{2+}$  salts according to literature [29]. The following reaction shows the magnetite forming reaction:



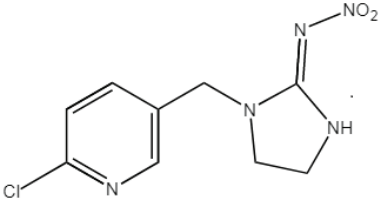
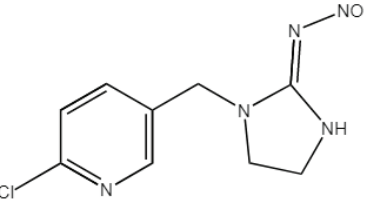
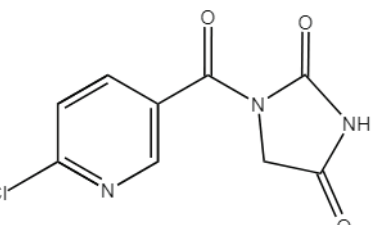
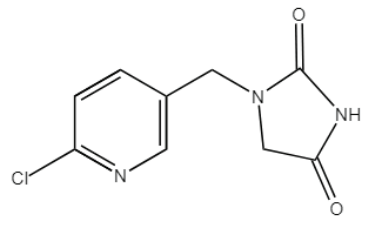
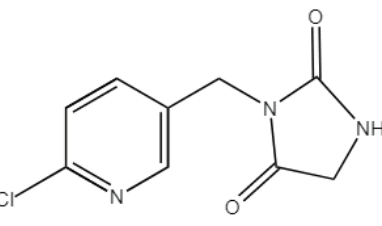
The black coloured magnetite particles were produced and precipitated in the reaction medium. The obtained magnetite particles were washed five times with water and dried at 65°C for 4 h in a vacuum oven.

### 2.3. Analysis methods of IMC

Quantitative analysis of IMC was carried out by using an Agilent 1200 Series HPLC system equipped with an ACE  $C_{18}$  column ( $250 \times 4.6$  mm, particle size 5  $\mu$ m). Using a mobile phase composed of water/acetonitrile (70:30, v/v) at a flow rate of 1 mL/min, the column temperature was 30°C and diode array detector (DAD) was operated with 270 nm. The calibration line was formed between 10 and 50 mg IMC/L ( $R^2 = 0.999$ ) at five points.

IMC degradation products were analyzed by LC/ESI-MS/MS. The Agilent LC/ESI-MS/MS system consists of a binary LC pump, an autosampler, and a temperature controlled column oven of Agilent series 1200 and an Agilent 6460 triple quadrupole mass spectrometer equipped with an electrospray ionization jet stream performance interface. Experimental conditions were as follows: drying gas ( $N_2$ , 20 psig) flow of 10 L/min, nebulizer pressure of 45 psig, drying gas temperature of 300°C and capillary voltage of

Table 1  
LC-ESI-MSMS data of imidacloprid degradation by nZVI in the nitrogen medium (50 mg IMC/L, 0.04 g nZVI/L, 25°C, pH 7.1)

Name and structure	Retention time (min)	Molecular mass and formula (g/mol)	Precursor ion (m/z)	Product ions (m/z)
1-[(6-Chloro-3-pyridinyl)methyl]- N-nitro-2-imidazolidinimine (imidacloprid)	12.75 (A)	255.7 C <sub>9</sub> H <sub>10</sub> ClN <sub>5</sub> O <sub>2</sub>	256–258	210, 175
				
1-[(6-Chloro-3-pyridinyl)methyl]- N-nitroso-2-imidazolidinimine (imidacloprid nitrosamine)	8.33 (B)	240.1 C <sub>9</sub> H <sub>10</sub> ClN <sub>5</sub> O	240–242	210, 175
				
3-(6-Chloropyridinyl)-(2,4-imidazolidindione)- ketone (imidacloprid urea ketone)	6.33 (C)	240 C <sub>9</sub> H <sub>8</sub> ClN <sub>3</sub> O <sub>2</sub>	238–240	209, 169
				
1-(6-Chloro-3-pyridylmethyl) imidazolidine- 2,4-dione (imidacloprid 4-keto urea)	5.80 (D)	225 C <sub>9</sub> H <sub>8</sub> ClN <sub>3</sub> O <sub>2</sub>	226–228	211, 169, 123
				
or				
1-(6-Chloro-3-pyridylmethyl) imidazolidine- 2,5-dione (imidacloprid 5-keto urea)				
				

2,000 V. The analytical separation was performed on an Agilent ACE-C18 column (4.6 × 150 mm, 5 μm) using isocratic elution of 70% H<sub>2</sub>O containing 0.1% FA and 30% CH<sub>3</sub>CN at a flow rate of 0.8 mL/min at 25°C. The MS detector was operated in the positive mode with mass detection in the range from 50 to 400 amu.

Dionex ICS-3000 ion Chromatography System, controlled by Chromeleon SE software was used for the analysis of released inorganic ions (Cl<sup>-</sup>, NO<sub>2</sub><sup>-</sup>, NO<sub>3</sub><sup>-</sup> and NH<sub>4</sub><sup>+</sup>) during the IMC treatment with nZVI. For anions analysis, anion-exchange column (IonPac AS9-HC, 25 cm × 4 mm) was linked to an IonPac AG9-HC, 5 cm × 4 mm column guard. For cations analysis, cation-exchange column (IonPac CS12A, 25 cm × 4 mm) was linked to an IonPac CG12A, 5 cm × 4 mm column guard. The system was equipped with a DS6 conductivity detector containing a cell heated at 35°C. An ASRS-ULTRA II (for anions) or CSRS-ULTRA II (for cations) self-regenerating suppressor was used to improve the sensitivity of the detector. A solution of 20 mM Na<sub>2</sub>CO<sub>3</sub> at 1.0 mL/min, and a 10 mM MSA solution at 1.0 mL/min were used as mobile phase for anion and cation analysis, respectively.

The mineralization efficiency of the IMC degradation was also determined with chemical oxygen demand (COD) analysis by using Lovibond COD LR test kits.

#### 2.4. Characterization methods of the nZVI

The scanning electron microscopy (SEM) images and energy dispersive X-ray (EDX) chemical analysis of nZVI were recorded with a Zeiss Supra 55 field emission SEM. The nZVI samples were coated under vacuum with platinum/palladium prior to the analysis to increase the surface conductivity.

The particle size distribution (PSD) of the nZVI was determined by using dynamic light scattering (DLS). The particles were dispersed in water with ultrasound equipment, then measured at 25°C, using a Malvern 2000 Zetasizer Nano ZS instrument with an angle of 90° (internal He-Ne laser, wavelength of 633 nm). Each sample was repeated at least six times for 1 mL suspension of samples at 0.1 g nZVI/L. The DLS data were evaluated with the Malvern Zetasizer 7.1 software package CW380 to yield the volume weighted size distributions of the assumed spherical particles. The volume distribution is frequently used to determine the modal particle diameter because it contains most of the particle volume.

X-ray diffractograms (XRD) of nZVI samples were performed using a Rigaku Smartlab model XRD at Cu-Kα radiation (λ = 1.54 Å). The analysis of dried nZVI was carried out in continuous scans from 10° to 100° at 2° scan rate at 2θ min<sup>-1</sup> in ambient air.

The fourier transform infrared spectroscopy (FTIR) measurements were also performed with Perkin Elmer/MIR spectrometer and a Pike Technologies Gladi ATR accessory. The FTIR spectra were obtained with the MIR mode at a constant ambient temperature of 25°C by accumulating 10 scans at a 1 cm<sup>-1</sup> resolution in the 4,000–450 cm<sup>-1</sup> region.

#### 2.5. Degradation experiments

The stock solution of IMC was prepared in 0.1 g/L concentration with ultra-pure water and used by diluting with

water in further experiments. Before the experiments, the desired pH of the solution was adjusted by Thermo Scientific Orion 4 Star digital pH meter with diluted H<sub>2</sub>SO<sub>4</sub> or NaOH solutions.

The degradation of IMC by nZVI was studied in both anoxic (nitrogen) and oxic (air) medium. After adding a desired amount of nZVI, the IMC solution was shaken in a thermostatically controlled shaker (Mettler Waterbath WHE-45). After that the nZVI nanoparticles were separated in the solutions by using SIGMA 3–30 K cooling centrifuge at 13,000 rpm. Then, the concentration of IMC in the solution was determined by using the HPLC system. The IMC degradation efficiency was calculated using the following equation:

$$\text{Removal}(\%) = \left( \frac{C_0 - C_t}{C_0} \right) * 100 \quad (3)$$

where Removal (%) was the IMC removal efficiency, C<sub>0</sub> (mg/L) was the initial IMC concentration and C<sub>t</sub> (mg/L) was the concentration of IMC at t min.

The effect of ions on the degradation of IMC was investigated with sodium salts for three different anions (NaCl, Na<sub>2</sub>SO<sub>4</sub> and Na<sub>2</sub>CO<sub>3</sub>). The salt concentration in the IMC solution was prepared to be 20 mg/L and the degradation experiments were carried out at 20°C, natural pH and initial IMC concentration of 30 mg/L.

Concentration of ferrous ions in IMC degradation solution was measured according to phenanthroline method using the UV–vis spectrophotometer [30]. Mohr's salt [FeSO<sub>4</sub>·(NH<sub>4</sub>)<sub>2</sub>SO<sub>4</sub>·6H<sub>2</sub>O] as Fe<sup>2+</sup> source, o-phenanthroline as complexing agent, CH<sub>3</sub>COONH<sub>4</sub> as buffer and NH<sub>4</sub>F for masking ferric ions were used. Ferric ion concentration in the degradation solution was determined by the reaction of Fe<sup>3+</sup> ions and salicylic acid forming a violet complex [31].

The reusability experiments were also performed in 10 cycles (0.1 g nZVI/L, initial IMC concentration of 50 mg/L, natural pH and 25°C). After each cycle, the reaction mixture was centrifuged to separate the nZVI from the reaction mixture and dried overnight in a vacuum oven at 105°C to be used again.

Aging test of nZVI under anoxic condition was prepared by putting fresh nZVI (0.1 g) into conical flask containing 50 mg/L of IMC solution. N<sub>2</sub> gas was continuously fed for 36 h at 25°C, natural pH. Samples were taken at 6, 12, 18, 24 and 36 h in the IMC solution for the measurement of iron ions. The nZVI sample was separated from the solution, dried and characterized.

### 3. Results and discussion

#### 3.1. Characterization of nZVI

The degradation of IMC by nZVI was carried out both in nitrogen and in air medium. After the degradation processes, nZVI samples were separated from IMC solutions, dried, labelled as nZVI/nitrogen and nZVI/air samples, respectively. All samples were characterized by XRD, SEM, EDX, DLS and FTIR analyses.

The XRD patterns of nZVI, nZVI/nitrogen and nZVI/air samples are illustrated in Figs. 1(a)–(c), respectively. Fig. 1(a) indicates that the typical characterization peak of

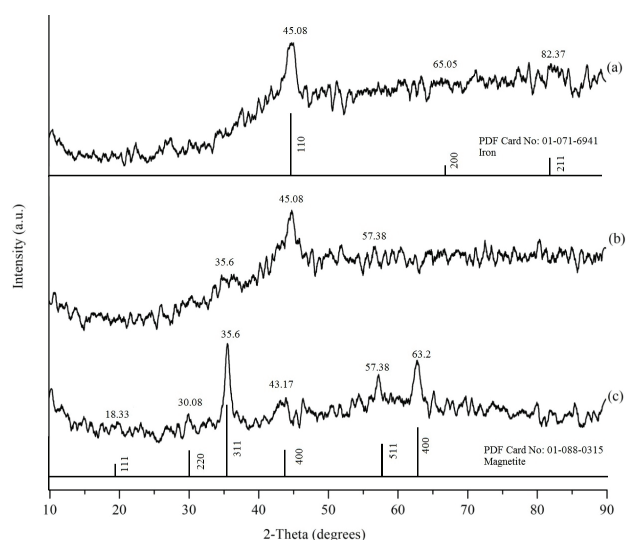


Fig. 1. XRD results of the nZVI samples for (a) pure nZVI, (b) nZVI/nitrogen and (c) nZVI/air (0.3 g nZVI/L, 30 mg IMC/L, pH 7.1, 20°C).

nZVI (a-Fe) at  $2\theta$  is about  $45.08^\circ$ . The similar peak was observed for the nZVI/nitrogen sample and also iron oxide peaks at low intensity ( $35.6^\circ$  and  $57.38^\circ$ ) were observed at the end of the 60 min treatment (Fig. 1(b)). These results show that the oxidation of nZVI was so slow in nitrogen medium for 60 min treatment. The XRD pattern of nZVI/air given in Fig. 1(c) belongs to the small signal intensity of nZVI at  $45.08^\circ$ , to the higher intensities of  $\text{Fe}_3\text{O}_4$  at  $2\theta$   $35.6^\circ$ ,  $63.2^\circ$  and also to the lower intensities at  $30.2^\circ$  and  $57.3^\circ$  [32–34]. But the presence of  $\gamma$ -FeOOH as an oxidation product was not observed. These results have shown that nZVI has oxidized to mainly magnetite in the air medium.

Figs. 2(a)–(c) show both the PSDs and SEM images of pure nZVI, nZVI/nitrogen and nZVI/air samples, respectively. For PSD results, the mean diameters were determined as 20.79 nm (standard deviation 1.489 d nm), 52.01 nm (standard deviation 6.017 d nm) and 92.72 nm (standard deviation 1.489 d nm), respectively (Figs. 2(a)–(c)). Thereby, the PSD results have shown that all nZVI samples are of nanoscale diameter. But mean diameter of nZVI/air sample is higher than those of the nZVI/nitrogen sample. The reason of increased particle size might be the subsequently formed magnetite layer on the surface of the nZVI in the air medium. As can be seen in Fig. 2(a), pure nZVI has spherical- and chain-like structure and also minimum aggregation. For the nZVI/nitrogen sample, Fig. 2(b) shows that the nZVI characteristic structure is spherical and chain like and is not decomposed. It is also protected by nitrogen atmosphere and there is no gap between the particles. In Fig. 2(c), nZVI structure has decomposed and the particle spherical shape has partially corrupted out and its particle surface has lost homogeneity.

The results of EDX analysis of nZVI/nitrogen and nZVI/air samples are illustrated in Fig. 3. In resulting values from platinum and palladium coating were neglected and iron and oxygen values were recalculated. As can be seen in Figs. 3(a) and (b), for nZVI samples in pure and nitrogen

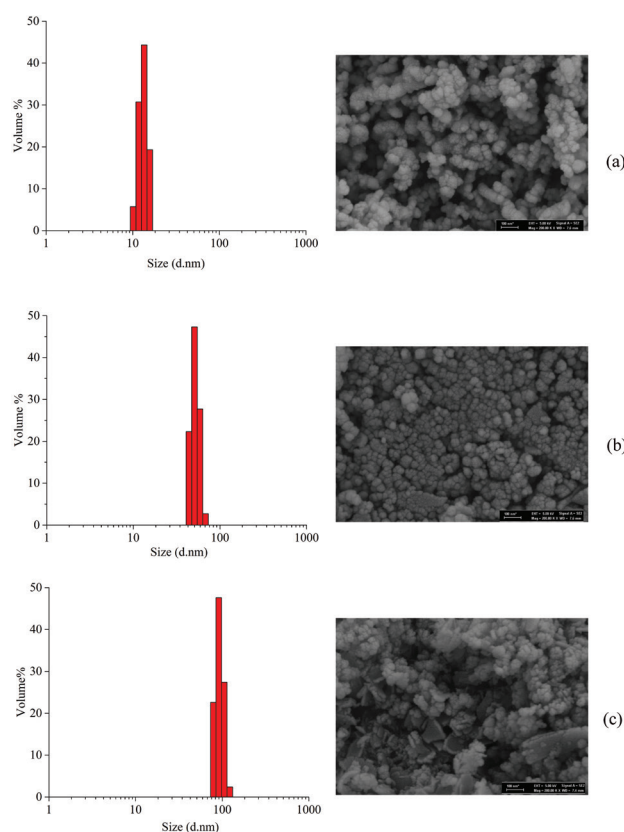


Fig. 2. SEM images and PSD results of the nZVI samples for (a) pure nZVI, (b) nZVI/nitrogen and (c) nZVI/air (0.3 g nZVI/L, 30 mg IMC/L, pH 7.1, 20°C).

medium, the main element is iron with a high percents (98.81% and 97.48%), and the percentages of oxygen are very low (1.19% and 2.52%), respectively. According to these results, it can be said that nZVI sample is slightly oxidized in nitrogen medium after 60 min treatment. Fig. 3(c) also shows the EDX results in air medium, that even though the main element is iron, its percentage is fairly low (61.98%) and the oxygen level is also very high (38.02%) when compared with in nitrogen medium.

Fig. 4 shows the FTIR spectra of pure nZVI ( $\text{Fe}^0$ ), pure IMC, nZVI samples treated with IMC both, in the nitrogen (nZVI/nitrogen) and in the air (nZVI/air) medium. The strong band observed at  $562\text{ cm}^{-1}$  for nZVI/air sample belongs to the stretching vibration mode of Fe–O bonds. Generally, the bands observed at about  $1,623$  and  $600\text{ cm}^{-1}$  show the presence of  $\text{Fe}_3\text{O}_4$  [19]. The Fe–O stretching vibration band was observed at  $562\text{ cm}^{-1}$  in the nZVI/air sample, not prominently observed in nitrogen medium for the end of the 60 min treatment. This result is consistent with the XRD analysis. Thus, it can be said that nZVI can be used repeatedly for the reactions carried out in the nitrogen medium. The FTIR spectrum of the pure IMC shows the peaks at  $3,076$ ,  $3,048$  and  $2,895\text{ cm}^{-1}$  bands corresponding to saturated and unsaturated C–H stretching. The peak at  $3,368\text{ cm}^{-1}$  band in the IMC corresponds to the symmetric stretching vibrations of N–H and the peaks at  $1,550$ – $1,566\text{ cm}^{-1}$  bands are the C=C and  $\text{NO}_2$  stretching frequencies. These peaks were not observed at

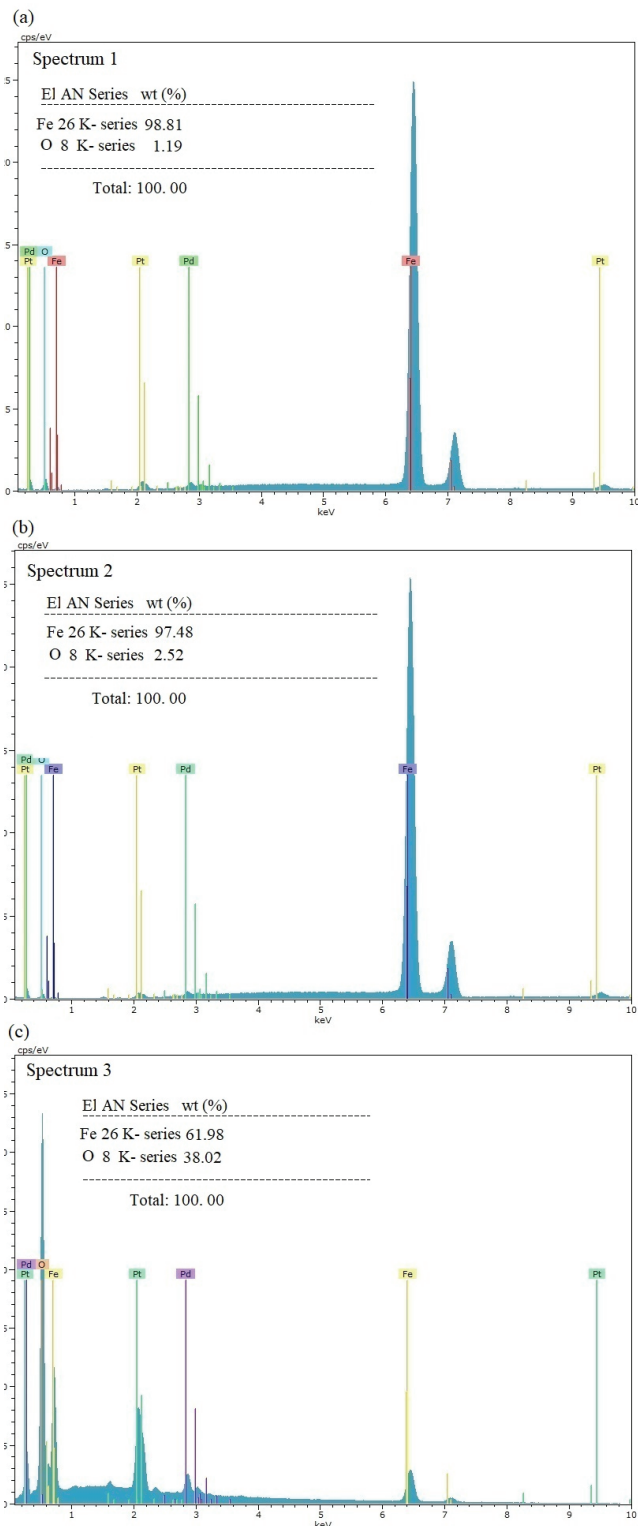


Fig. 3. EDX results of the nZVI samples for (a) pure nZVI, (b) nZVI/nitrogen and (c) nZVI/air (0.3 g nZVI/L, 30 mg IMC/L, pH 7.1, 20°C).

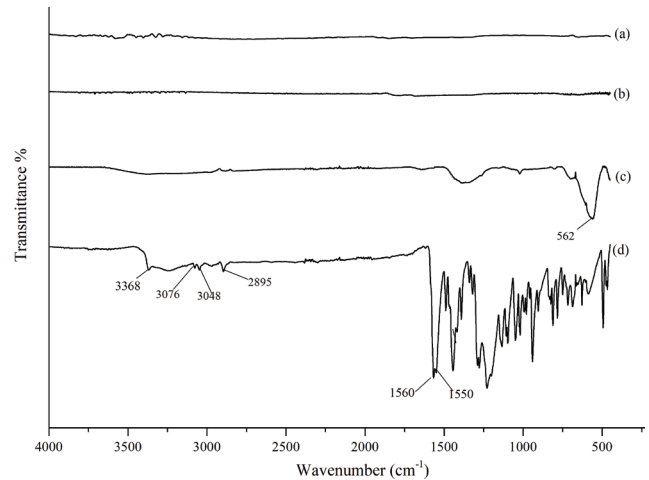


Fig. 4. FTIR spectra of (a) pure nZVI, (b) nZVI/nitrogen, (c) ZVI/air and (d) pure imidacloprid (0.3 g nZVI/L, 30 mg IMC/L, pH 7.1, 20°C).

nZVI/nitrogen and nZVI/air samples (Fig. 4). These results suggest that IMC is not adsorbed by nZVI or oxidation product ( $\text{Fe}_3\text{O}_4$ ) in the air or the nitrogen medium, it is only degraded by the nZVI treatment.

### 3.2. Degradation of IMC by nZVI

#### 3.2.1. Effect of the nitrogen and the air medium on IMC degradation at different nZVI amounts

Degradation experiments were conducted both in anoxic condition by feeding nitrogen as an inert gas to the reaction medium and also in oxic condition where the experiments took place in an air environment. At all stages of this study, HPLC-DAD was used to observe the change in initial concentrations of IMC with time both in the air and the nitrogen medium. As shown in the HPLC results in Figs. 5(a) and (b), the retention time of IMC was determined about 6.1 min, both in the air and the nitrogen medium. A peak of the IMC metabolite was clearly observed about 4.1 min in the nitrogen medium, but this metabolite peak was observed to be at a low level in the air medium (50 mg IMC/L and 0.04 g nZVI/L). But the intensity of this peak was increased at higher nZVI loadings, both in the nitrogen and in the air medium. The observed peak at 4.1 min showed that IMC was more effectively degraded in the nitrogen medium than in the air. Unfortunately, it was not possible to detect the metabolites during the degradation period by nZVI using HPLC-DAD without appropriate standards of IMC metabolites. These possible metabolites were identified using LC-ESI-MS/MS (Fig. 9).

In order to determine the effect of nitrogen and air environment for the IMC degradation, different amounts of nZVI were used for the air medium (0.20, 0.30 and 0.60 g/L) and the nitrogen medium (0.20, 0.30 and 0.60 g/L) for 30 mg/L initial IMC concentrations. The obtained results are given in Fig. 6 and Table 2.

The results showed that the IMC removal percentages for studied amounts in the nitrogen medium were higher than

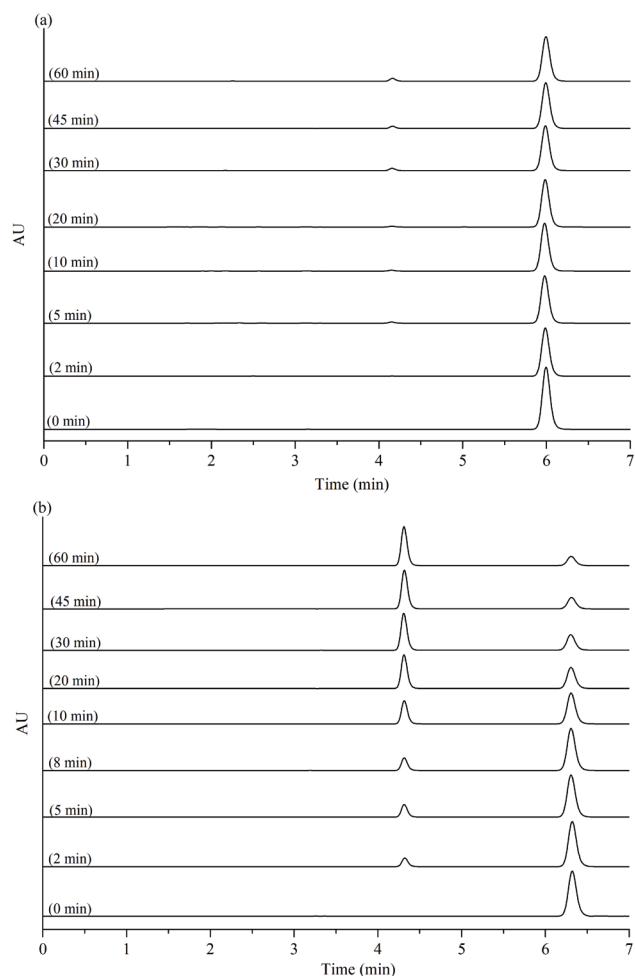


Fig. 5. HPLC chromatograms of imidacloprid degradation by nZVI in (a) air and (b) nitrogen medium (0.04 g nZVI/L, 30 mg IMC/L, pH 7.1, 20°C).

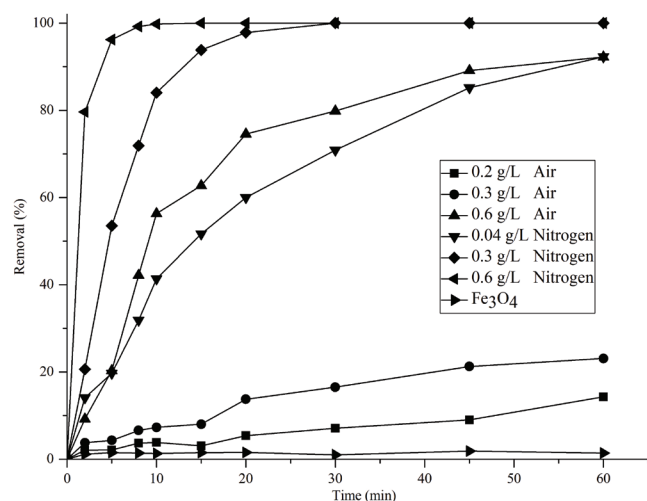


Fig. 6. Removal efficiencies of imidacloprid for different nZVI amounts in nitrogen/air mediums and  $\text{Fe}_3\text{O}_4$  (30 mg IMC/L, pH 7.1, 20°C).

Table 2

First-order rate constants ( $k_1$ ) and regression coefficients ( $R^2$ ) for the degradation of imidacloprid by zero valent iron nanoparticles for different parameters

Parameters	$k_1$ ( $\text{min}^{-1}$ )	$R^2$	Removal %
<i>nZVI amount (g/L in nitrogen)</i>			
0.04	0.0416	0.997	92.28
0.30	0.1955	0.995	99.00
0.60	0.5943	0.996	100.00
<i>nZVI amount (g/L in air)</i>			
0.20	0.0022	0.956	14.30
0.30	0.0044	0.951	23.10
0.60	0.0435	0.952	92.24
<i>pH</i>			
3.0	0.0077	0.911	36.56
7.1	0.0416	0.997	92.28
10.0	0.0226	0.977	74.44
<i>T (°C)</i>			
20	0.0416	0.997	92.28
25	0.0673	0.993	98.44
30	0.1189	0.994	99.00
40	0.1736	0.997	100.00

Experimental conditions for temperature ( $T$ ):  $m_{\text{nZVI}} = 0.04$  g/L,  $C_{0,\text{IMC}} = 30$  mg/L, pH = 8; for initial imidacloprid concentration ( $C_{0,\text{IMC}}$ ):  $m_{\text{nZVI}} = 0.04$  g/L,  $T = 20^\circ\text{C}$ , pH = 8; for amount of (nZVI  $m_{\text{nZVI}}$ ):  $C_{0,\text{IMC}} = 30$  mg/L,  $T = 20^\circ\text{C}$ , pH = 8; for pH:  $C_{0,\text{IMC}} = 30$  mg/L,  $m_{\text{nZVI}} = 0.04$  g/L,  $T = 20^\circ\text{C}$

those of the air medium. For example, 0.30 and 0.60 g nZVI/L amounts in the nitrogen and the air medium, the removal percentages of IMC were obtained as 23.10% and 92.28% for the air medium and 99% and 100% for the nitrogen medium, respectively. These results demonstrated that the IMC degradation at anoxic condition by providing nitrogen was more effective than oxic condition.

In the air medium, since the nZVI surface is inactivated by the oxide layer, degradation process does not take place effectively. To avoid this problem an effective way should be applied to hinder the corrosion reaction. Thus, the degradation process of contaminant by using nZVI is generally implemented under fully anoxic conditions by the absence of oxygen gases [35]. It is seen that nZVI is a highly effective material for the removal of the IMC, especially in anoxic condition by providing nitrogen medium.

The results also showed that the increased nZVI amount enhanced the degradation efficiency of IMC, both in the nitrogen and in the air medium. The more nZVI particles will ensure the more surface sites in reaction medium that will accelerate the degradation. As can be seen in Fig. 6 and Table 2, for 30 mg/L initial IMC concentration, 92.28% and 99.00% of the IMC were removed for 0.04 and 0.3 g nZVI/L loadings in nitrogen medium within 60 min, respectively.

With the assumption that the degradation pathways followed first-order kinetics, the degradation rates of IMC were also determined for different nZVI amounts both in the air and in the nitrogen mediums and given in Table 2. In the nitrogen medium, the regression lines of first-order kinetics fitted better to the model with high correlation coefficients than in

the air medium at different amounts of nZVI. The increased nZVI amount in the degradation reactions enhanced the degradation efficiency. The degradation rate constants were determined as 0.0022, 0.0044, 0.0435  $\text{min}^{-1}$  for 0.2, 0.3, 0.6 g nZVI/L in the air medium and 0.0416, 0.1955, 0.5943  $\text{min}^{-1}$  for 0.04, 0.3, 0.6 g nZVI/L in the nitrogen medium, respectively. The obtained higher rate constants with the increasing nZVI amounts may be attributed to an increase of active sites and reactive surface areas on the ZVI, since the reaction has occurred at the nZVI–H<sub>2</sub>O interface [36]. Other researchers have also found a same trend in the degradation of azo dyes [18,37], 2,4,6-trinitrotoluene [38], hexachlorobenzene [37] and lindane [39] by using various amounts of nZVI. As can be seen in Table 2, the obtained rate constants in nitrogen medium were also higher than those of the air medium. As a conclusion, the degradation of IMC in the nitrogen medium was quite effective than in the air medium.

### 3.2.2. Effects of pH in nitrogen medium

The degradation of IMC by nZVI in the nitrogen medium was studied at pH 3 (acidic), pH 7.1 (original solution pH), pH 10 (basic) and the removal efficiencies and calculated first-order rate constants are given in Fig. 7 and Table 2, respectively. The results showed that pH of the IMC solution strongly affected the degradation efficiencies and rates. As can be seen in Fig. 7, IMC degradation efficiency is higher in near neutral pH (also original solution pH) than in acidic and basic solution pHs. For example, when the nZVI amount was constant at 0.04 g/L, the rate constants and removal efficiencies of 30 mg IMC/L solution at pHs 3.0, 7.1 and 10.0 were obtained as 0.0077, 0.0416, 0.0226  $\text{min}^{-1}$  and 36.56, 92.28, 74.44%, respectively (Table 2). Therefore, results showed that the IMC degradation was much more effective in neutral pH than in basic and especially in acidic pHs.

The pH of the reaction medium can affect the performance of the ZVI by accelerating the corrosion of iron at low pH, and passivating it by the formation of iron hydroxides at high pH [10,40]. At low pH, the activity of protons is high.

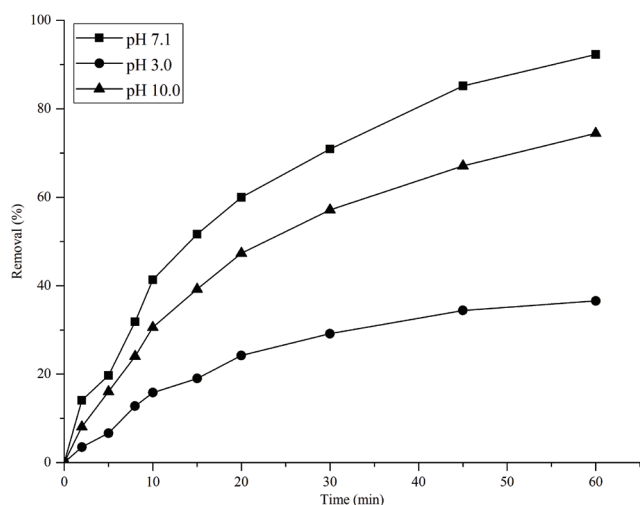


Fig. 7. Removal efficiencies of imidacloprid degradation by nZVI for different pH values in the nitrogen medium (0.04 g nZVI/L, 30 mg IMC/L, 20°C).

Protons readily accept electrons from ZVI, resulting in the formation of corrosion products on the ZVI surface. By the formation of corrosion reaction, nZVI turns in as less electron donor for IMC degradation [10,17,41],  $\text{Fe}^{2+}$  can be the major redox active ion in corrosion of nZVI for this system [41]. The released ferrous ions will precipitate as  $\text{Fe}(\text{OH})_2$  due to its low solubility ( $K_{\text{sp}} = 8.0 \times 10^{-16}$  at 25°C) [40]. This can be further oxidized to different Fe(II, III) oxide compounds such as magnetite, lepidocrocite, ferrihydrite and goethite, which cover the surface of the ZVI (Eqs. (6)–(10)). It is also apparent that the degradation of IMC was inhibited in alkaline condition because of auto oxidation of nZVI and the changing of surface charge of nZVI. As a result, further reactions between nZVI and the IMC will be prevented by the inactivated nZVI surface [10,17,41,42].

### 3.2.3. Effect of temperature

Effect of temperature on IMC degradation by nZVI in the nitrogen medium was investigated for 20°C, 25°C, 30°C and 40°C temperature values. The changing of removal efficiencies of IMC with time for different temperature values are given in Fig. 8. The results showed that the IMC removal percentages increased with increasing solution temperature as 92.28%, 98.44%, 99.00% and 100.00% for these temperature values, respectively (Table 2).

The first-order reaction rate constants ( $k_1$ ) were obtained with a correlation coefficient ( $R^2$ ) of more than 0.993 values as 0.0416, 0.0673, 0.1189 and 0.1736  $\text{min}^{-1}$  for 20°C, 25°C, 30°C, 40°C, respectively (Table 2). The results indicated that the degradation of IMC was affected by temperature and the rate constants increased from 293 to 313 K nearly four times.

The degradation process of IMC proved to be an endothermic reaction because the first-order rate constants values also increased as the temperature increased. The activation energy in the range of 20°C–40°C was found by applying the Arrhenius equation [17] with the high correlation coefficient

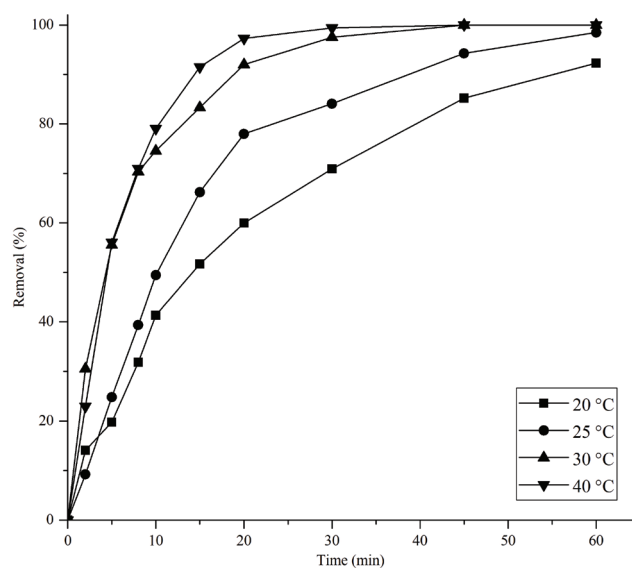


Fig. 8. Removal efficiencies of imidacloprid degradation by nZVI for different temperature values in the nitrogen medium (0.04 g nZVI/L, 30 mg IMC/L, 20°C, pH 7.1).

( $R^2=0.915$ ). A more than 42.0 kJ/mol magnitude of  $E_a$  implies a surface-limiting reaction [43,44]. The  $E_a$  value was calculated as 54.68 kJ/mol indicating that the dominating degradation reactions of IMC took place on the surface of nZVI.

### 3.3. Degradation pathway of IMC by ZVI

Although different methods such as photocatalytic degradation, photodegradation and ozonation and also different intermediates have been given in the literature for the degradation of IMC [1,6,45–49], there is a limited number of studies working with nanoparticles and also with ZVI. In  $Fe^0/H_2O$  systems, water is present in stoichiometric abundance (solvent), and is corrosive to  $Fe^0$  (nZVI) both under oxic and anoxic conditions [50].

Under oxic condition,  $Fe^0$  is predominantly corroded by oxygen to  $Fe^{2+}$  (Eq. (4)) [48,49]. Also, further oxidation of  $Fe^{2+}$  to  $Fe^{3+}$  may result in generation of different iron oxides ( $Fe_3O_4$ ,  $Fe_2O_3$ ,  $Fe(OH)_3$ ,  $FeOOH$ ) (Eqs. (5), (8) and (9)). These oxide species cover the surface of the nZVI and decrease its activity [15,35,52].

As confirmed by XRD results, magnetite ( $Fe_3O_4$ ) forms as a main oxide form by the treatment of nZVI with IMC in air medium (Fig. 1). These results show that the oxygen in water and in the air medium leads to oxidation of the surface. Therefore, the surface is inactivated by the oxide layer thus degradation process does not take place effectively. On the other hand, some researchers have shown that some substances can be adsorbed by the passive iron oxide layers [10,53]. In this study, to determine whether the IMC could be adsorbed by magnetite or not,  $Fe_3O_4$  nanoparticles were synthesized and treated with IMC like in the treatment process of the nZVI procedure in the air medium. The results are given in Fig. 6. As can be seen in this figure, IMC has not been adsorbed on the nZVI surface. This has proved that the IMC removal resulting in the air medium has provided only by the degradation process without any of adsorption.

Under anoxic condition, when nZVI ( $Fe^0$ ) reacts with water,  $Fe^0$ ,  $H^+$  and  $OH^-$  ions are generated (Eq. (6)).  $Fe^{2+}$  can take up  $OH^-$  ions and then the first corrosion products of  $Fe(OH)_2$  and  $Fe(OH)_3$  are produced and also both of which can turn  $FeOOH$ ,  $Fe_2O_3$  and  $Fe_3O_4$  (Eqs. (8)–(10)) [51,53,54]. These iron oxides may mask the redox active sites of the  $Fe^0$  where exchange of electrons between  $Fe^0$  and contaminants is facilitated [52,57].



As soon as  $Fe(OH)_2$  and  $Fe(OH)_3$  start to precipitate on nZVI particles they inevitably adsorb  $Fe^{2+}$  forming continuously by corroding of  $Fe^0$ . This adsorbed  $Fe^{2+}$  ( $Fe_{(ads)}^{2+}$ ) yields the more contaminant reduction [52,51,54]. In fact, in  $Fe^0/H_2O$  systems, contaminant removal is not only provided by the  $Fe^0$  reactivity (reduction by electrons from  $Fe^0$ ) but also corrosion products are not inert, they actively participate to contaminant removal [38,54]. Many researchers have pointed out that contaminant removal could be mostly associated with primary ( $Fe^{2+}$ ,  $Fe_{(ads)}^{2+}$ ,  $H/H_2$ ) and secondary (iron hydroxides and oxides) iron corrosion products for a  $Fe^0/H_2O$  system [50,55,57]. The standard reduction potential of  $E^0_{Fe(II)/Fe(0)}$  and  $E^0_{Fe(III)/Fe(II)}$  is  $-0.44$  V and  $-0.35$  to  $-0.65$  V, respectively [58]. From the thermodynamic perspective, these reduction potential values suggests that, in some circumstances ( $E^0 < -0.44$  V), contaminant reduction by  $Fe^{2+}$  and also  $Fe_{(ads)}^{2+}$  might be more favourable than reduction by electrons from  $Fe^0$  [50,57].

Degradation reaction of organic compounds by using nZVI occurs on the surface of metal particles. When nZVI particles contact with organic molecules, iron acts as an electron donor and organic molecules act as an electron acceptor [45]. IMC accepts electrons from nZVI and turns into the transitional products and then final products. Although nZVI corrosion can take place both in oxic and in anoxic conditions in aqueous solutions, the results show highly inactivation of the nZVI in oxic condition because of the fast oxidation of nZVI in air medium. The reason for high-level IMC degradation efficiency in anoxic condition may be due to the effectiveness of primary and secondary corrosion products than oxic condition.

In the nitrogen medium, the degradation products of IMC were identified by LC-ESI-MS/MS and chromatograms for 0, 2, 30 and 60 min are given in Fig. 9 and the observed data are also summarized in Table 1.

The IMC peak was observed at 12.75 min (compound A) in the control sample (at 0 min) (Fig. 9(a)) and this peak fragments are presented in Table 1. Precursor ion and characteristic product ions of IMC were confirmed  $m/z$  256.1 (A+H), 210 [A+H-NO<sub>2</sub>] and 175 [A+H-NO<sub>2</sub>-Cl<sup>-</sup>], respectively. And similar fragments for IMC were also reported by Žabar et al. [4] and Bourgin et al. [49]. In Figs. 9(b)–(d), it was observed that the IMC peak area decreased after 2 min and then disappeared within 30 and 60 min.

Three main compounds (B, C and D) corresponding to the degradation products of IMC were detected at 8.28, 6.33 and 5.80 min, respectively (Figs. 9(b)–(d)). The molecular weight of these compounds was confirmed by LC-ESI-MS/MS as 240, 238 and 226 g/mol, respectively. The LC-ESI-MS/MS data of these products were given in detail in Table 1. These intermediates of IMC were given in the literature for different degradation methods such as ozonation, photocatalytic and nanoparticles [4,49,59–61]. When the results were evaluated, compound B was identified as IMC nitrosamine (1-(6-chloro-3-pyridylmethyl)-nitrosoimidazolidin-2-ylideneamine) with the characteristic precursor ion  $m/z$  = 240–242 [B+H] and product ion peaks at  $m/z$  210 [B+H-NO], 194 [B+H-NO<sub>2</sub>] and 175 [B+H-NO-Cl<sup>-</sup>]; compound

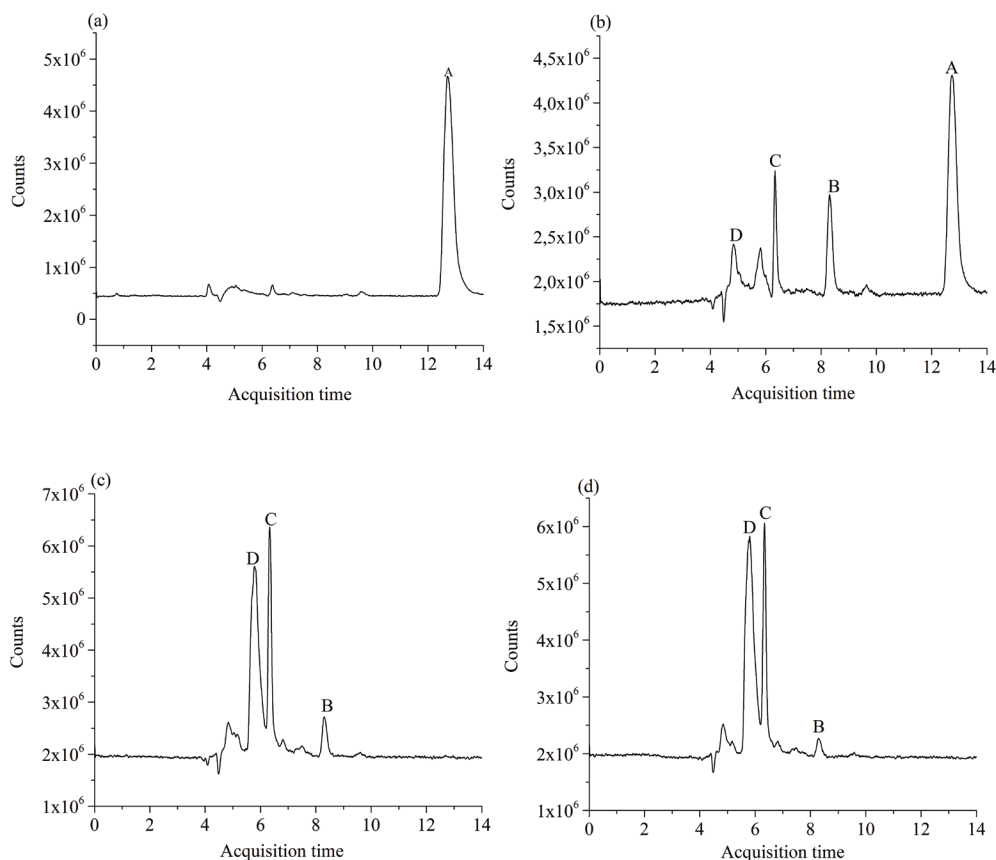


Fig. 9. LC-ESI-MS/MS chromatograms of imidacloprid and degradation products by nZVI in the nitrogen medium for (a) 0 min, (b) 2 min, (c) 30 min and (d) 60 min (30 mg IMC/L, 0.04 g nZVI/L, 25°C, pH 7.1).

C was identified as IMC urea ketone (3-(6-chloropyridinyl)-(2,4-imidazolidindione)-ketone) with the characteristic precursor ion peaks  $m/z = 238-240$  [C + H] and product ion peaks at  $m/z$  209 [C+H-O<sub>2</sub>] and 169[C+H-C<sub>2</sub>H<sub>3</sub>O<sub>2</sub>N]; and also compound D was identified as IMC keto urea with the characteristic precursor ion peaks  $m/z = 226-228$  [D+H] and product ion peaks at  $m/z$  211 [D+H-O] and 169 [D+H-C<sub>2</sub>H<sub>3</sub>NO], respectively. According to these results, a possible degradation pathway of IMC by using nZVI was proposed and is given in Fig. 10.

Also, to evaluate and determine the level of the IMC mineralization by nZVI in the nitrogen medium, COD and released inorganic ions were analyzed during the degradation time at 0.24 g nZVI/L and 50 mg IMC/L IMC concentration and the results are given in Figs. 11(a) and (b), respectively. The COD changes were determined at different time intervals of degradation for 300 min and given in Fig. 11(a). While the initial COD amount of IMC was 72 mg/L, the value decreased to 63 mg/L after 300 min of degradation time. As a result, the efficiency of COD removal was 12.5%.

During the degradation process of IMC by nZVI in the nitrogen medium, the evaluation of released inorganic ions was followed by IC analysis. The amount of Cl<sup>-</sup> can give information about the maximum mineralization level. IMC chemical structure includes one Cl and five N atoms, theoretically

the maximum limits of Cl<sup>-</sup> and N, released into the solution, were 6.94 and 13.67 mg/L, respectively. As can be seen in Fig. 11(b), at the end of 300 min, a low increase in the amount of chlorine ions confirms that the level of mineralization is low (measured realized amount of Cl<sup>-</sup> is 0.24 mg/L). But, the NO<sub>2</sub><sup>-</sup>, NO<sub>3</sub><sup>-</sup> and NH<sub>4</sub><sup>+</sup> results are insufficient to determine the maximum mineralization of IMC degradation by nZVI (Fig. 11(b)). Because it is unclear in what kind of ions the nitrogen atoms in the IMC structure transform during the degradation process. Even, the nitrogen atoms, N<sub>2</sub> or N<sub>x</sub>O<sub>y</sub> have the potential to transform into one of the gas forms [62]. The NO<sub>2</sub><sup>-</sup>, NO<sub>3</sub><sup>-</sup> and NH<sub>4</sub><sup>+</sup> values were measured as 0.27, 0.31 and 0.18 mg/L, respectively, after 300 min degradation. In summary, COD and ion measurement results indicate that the mineralization of IMC by nZVI in nitrogen medium is very low.

#### 3.4. Effects of anions

Degradation of IMC by nZVI in anoxic condition may be affected by the presence of other ions in the water. Therefore, the effects of three anions (Cl<sup>-</sup>, CO<sub>3</sub><sup>2-</sup> and SO<sub>4</sub><sup>2-</sup>) were investigated separately at natural pH and 20 mg/L concentrations of each anion salt. The first-order kinetic rate constants and

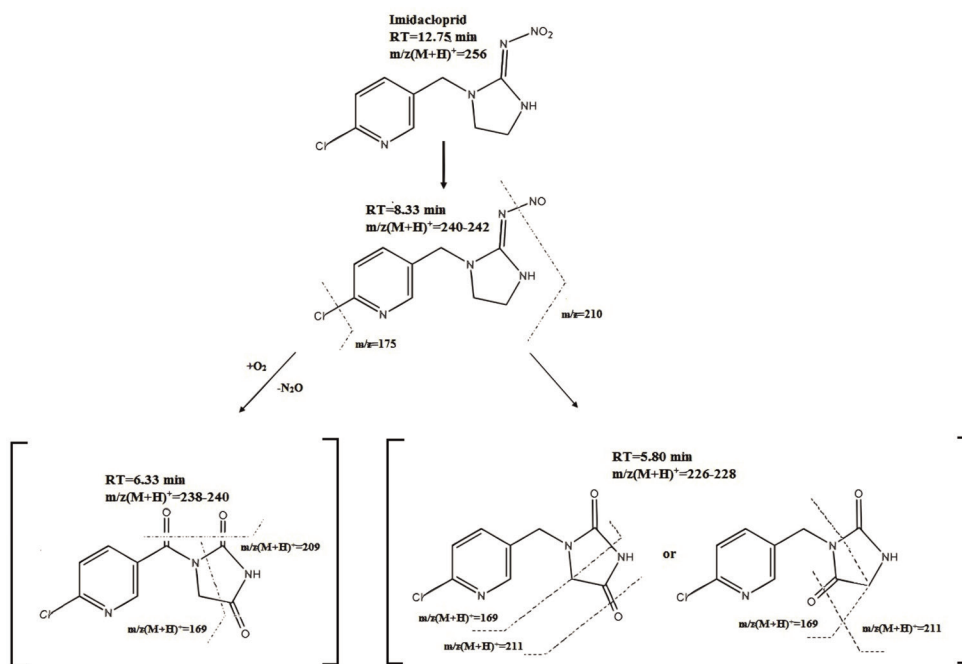


Fig. 10. Possible degradation pathway of imidacloprid.

the percent IMC removal results are given in Table 3. The removal efficiency of IMC in the presence of anion decreased from 91.8% to 91.2%, 90.5% and 89.9% for chloride, carbonate and sulphate, respectively. The presence of anions may prevent to contact of IMC with the active sites of the nZVI surface. Therefore, IMC removal percentages and rate constants reduced slightly in the presence of anions.

Table 3  
Percent of IMC removal and first-order kinetic rate constants in the presence of anions (30 mg IMC/L, 20°C, natural pH, 0.04 g nZVI/L)

Anions	IMC removal (%)	Rate constant ( $K_1$ ) ( $\text{min}^{-1}$ )
Sulphate	89.9	0.0401
Carbonate	90.5	0.0403
Chloride	91.2	0.0408
Without anions	91.8	0.0416

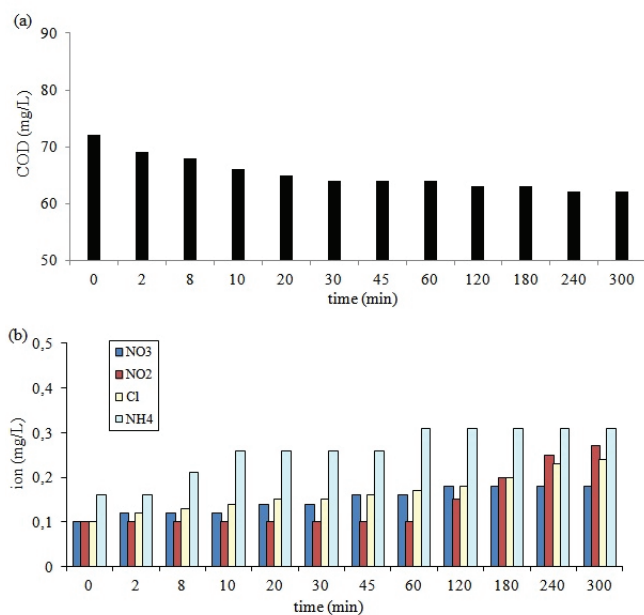


Fig. 11. Evaluation of (a) COD and (b) released inorganic ions results during the degradation of imidacloprid in the nitrogen medium (0.24 g nZVI/L, 50 mg IMC/L, pH 7.1, 25°C).

### 3.5. Reusability of nZVI

It is important economically to be able to reuse nZVI in removing pollutants from aqueous solutions. The reusability of nZVI and also  $\text{Fe}^{+2}$  and  $\text{Fe}^{+3}$  ions which were leached from nZVI were investigated for IMC degradation and 10 cycles reusability results shown in Fig. 12 were obtained. After 10 cycles, removal efficiency of IMC decreased from 100% to 89%. These results showed that nZVI could be efficiently reused for in the degradation of IMC in nitrogen (anoxic) medium. The slight decrease in the removal efficiency of IMC during the recycling may be due to the loss and little oxidation of nZVI in the separation process.

The concentrations of the  $\text{Fe}^{+2}$  and  $\text{Fe}^{+3}$  ions in the degradation solutions were determined to be lower than 0.2 and 0.5 mg/L, respectively. The obtained high percent IMC removal results under anoxic condition show that the reaction rate between nZVI and water is slow [44] and also the released  $\text{Fe}^{+2}$  and  $\text{Fe}^{+3}$  ions at low level probably turn to

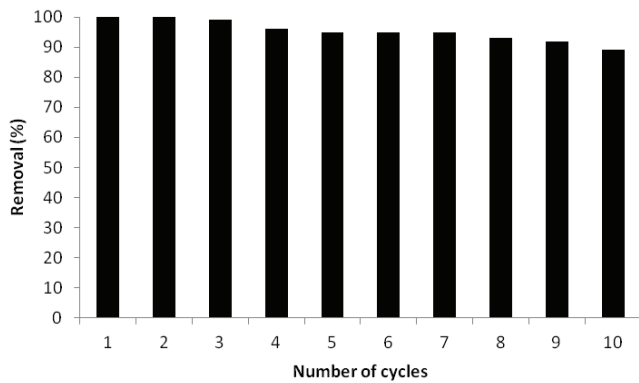


Fig. 12. Recycling efficiency of nZVI for degradation of IMC in nitrogen medium (0.1 g nZVI/L, 50 mg IMC/L, 25°C, natural pH).

corrosion products or be adsorbed on corrosion products. At the end of 10 cycles, XRD and FTIR measurements of treated nZVI in nitrogen medium confirmed that magnetite formed on the nZVI surface (Fig. 13).

As a result of FTIR, the Fe–O stretching vibration band was observed at 562  $\text{cm}^{-1}$  in Fig. 13(a). This most basic peak indicating that nZVI oxidized is more severe at the end of 10th cycle than in after 36 h.

Characteristic peaks of  $\text{Fe}_2\text{O}_3$  and  $\text{Fe}_3\text{O}_4$  were observed at 30.2°, 35.6°, 57.2° and 62.7° in the XRD spectrum (Fig. 13(b)). And also EDX analyses of treated nZVI after 10 cycles are illustrated in Fig. 13(c). According to EDX results percentage of oxygen element increased from 2.52% (Fig. 13(b), in nitrogen medium for 60 min treatment) to 15.57% (Fig. 13(c)). These results show that nZVI is slightly oxidized at the end of 10 cycles in nitrogen medium.

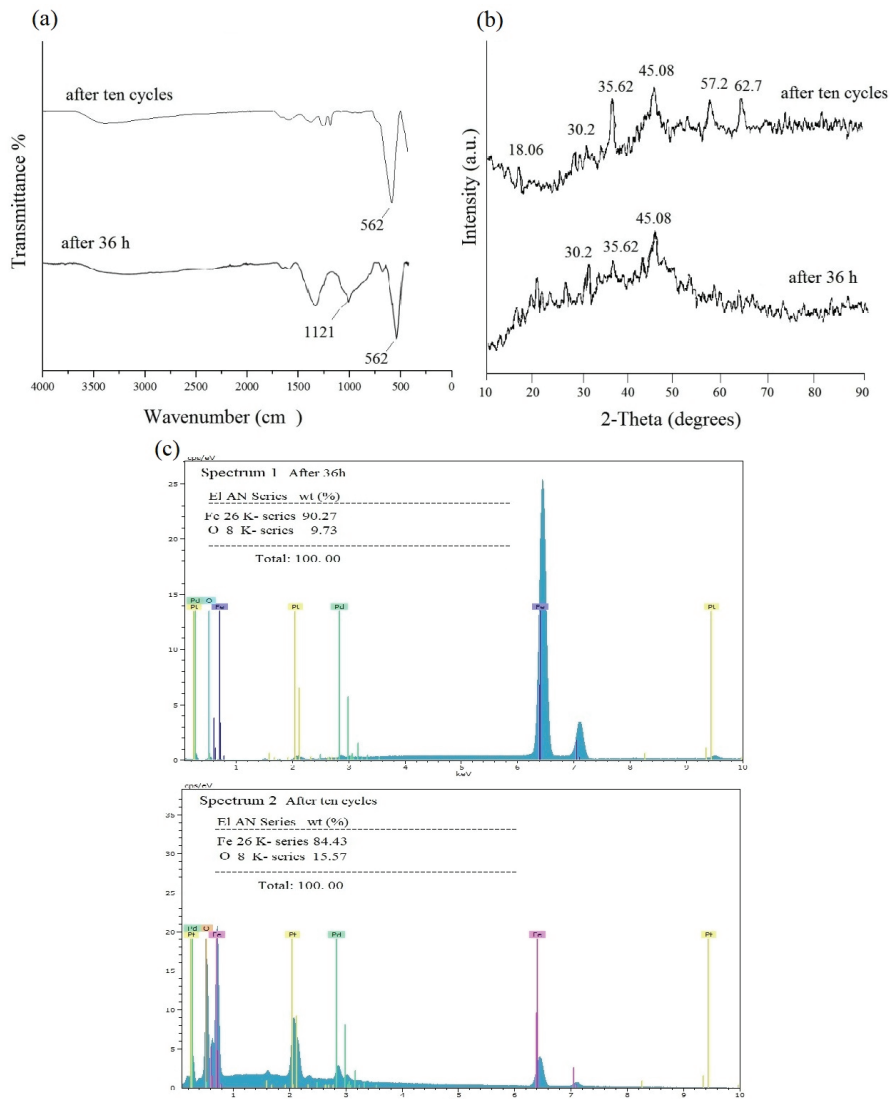


Fig. 13. FTIR (a), XRD (b) and EDX (c) results of nZVI after 10 cycles and after 36 h in the degradation of IMC (0.1 g nZVI/L, 50 mg IMC/L, 25°C, natural pH).

### 3.6. Aging test of nZVI

The nZVI aged in the IMC solution for 36 h in the nitrogen medium was analyzed with XRD, FTIR and SEM (Figs. 13(a)–(c)). In Fig 13, XRD, SEM and FTIR results indicated that nZVI was oxidized after 36 h in the IMC degradation solution. In Fig. 13, according to XRD, SEM and FTIR results, after 36 h the nZVI was less oxidized than end of the 10th cycle. In the XRD results, characteristic  $\text{Fe}_2\text{O}_3$ ,  $\text{Fe}_3\text{O}_4$  ( $30.2^\circ$ ,  $35.6^\circ$ ) peaks as well as nZVI peak ( $45.08^\circ$ ) were observed. The intensity of the characteristic peak at  $2\theta$  of  $45^\circ$  indicates that the ZVI is still dominantly present in the sample. The concentrations of  $\text{Fe}^{2+}$  and  $\text{Fe}^{3+}$  in the IMC solution were also determined for 6, 12, 18, 24, 36 h and given in Table 4. After 36 h, the leached of  $\text{Fe}^{2+}$  and  $\text{Fe}^{3+}$  remained at very low values of 0.43 and 0.60 mg/L, respectively. These results indicated that nZVI was well protected, oxidation rate of nZVI was low and the low level of released  $\text{Fe}^{2+}$  and  $\text{Fe}^{3+}$  might have been adsorbed by the corrosion product in the nitrogen medium. Liu et al. [54] also worked on nZVI evolution in the nitrogen medium and have shown that nZVI is slightly oxidized after 72 h.

### 4. Conclusions

IMC can pose a significant hazard with the unused amount that is involved in the environment because of extensive use. In this study, nZVI was synthesized, characterized and used to remove IMC, both in air and in nitrogen medium. The XRD and FTIR measurements indicated that the typical characterization peak of nZVI was not changed significantly in anoxic (nitrogen) medium at the end of the 60 min IMC treatment but an additional prominent peak of magnetite was observed in the oxic (air) medium, showing the oxidation of nZVI particles. SEM results also showed that the structures were decomposed in the air medium, but its spherical and homogeneous shape was protected in the nitrogen medium. The increase of the particle size in the air medium might be because of formed magnetite layer on the surface of the particle that affects the degradation efficiency.

The effects of nZVI dosage, pH and temperature were also investigated in the nitrogen medium and degradation rate constants ( $k_d$ ) were determined by using the first-order kinetics model. The increased nZVI amount enhances the active sites and reactive surface areas of the ZVI and also the degradation efficiency of IMC. Lower IMC removal efficiencies were obtained at the higher pH and especially at the lower pH values compared with original pH of IMC.

Table 4

Concentration of  $\text{Fe}^{2+}$  and  $\text{Fe}^{3+}$  ions in the aged nZVI solution (nitrogen medium, 0.1 g nZVI/L, 50 mg IMC/L, 25°C, natural pH)

Time (h)	$\text{Fe}^{2+}$ (mg/L)	$\text{Fe}^{3+}$ (mg/L)
0	<0.2	<0.5
6	0.29	<0.5
12	0.29	0.55
18	0.35	0.58
24	0.44	0.58
36	0.43	0.60

Because at low pH the corrosion of iron accelerates and is passivated by the formation of iron hydroxides at high pH. The temperature effect was investigated for 20°C, 25°C, 30°C and 40°C temperature values and IMC removal percentages increased to 92.28%, 98.44%, 99.00% and 100.00% with increasing solution temperature, proving to be an endothermic reaction. Also, the rate constants increased from 20°C to 40°C nearly four times. The activation energy ( $E_a$ ) value was calculated as 54.68 kJ/mol indicating that the dominating degradation reactions of IMC took place on the surface of nZVI.

The level of the IMC mineralization was also investigated by COD and released inorganic ions measurements. The results showed low mineralization efficiency as 12.5% COD removal. The degradation products of IMC were identified by LC-ESI-MS/MS analysis. The three main compounds determined by this analysis were IMC nitrosamine, IMC urea ketone and IMC keto urea. According to these results a possible degradation mechanism was proposed for IMC degradation by using nZVI. The presence of  $\text{Cl}^-$ ,  $\text{CO}_3^-$  and  $\text{SO}_4^{2-}$  anions in the aqueous solution of IMC affected slightly the removal efficiency of IMC. The aging and reusability tests of nZVI also showed that nZVI can be used repeatedly as an efficient material in the nitrogen medium because of the low oxidation of nZVI.

### References

- [1] V. Kitsiou, N. Filippidis, D. Mantzavinos, I. Poullos, Heterogeneous and homogeneous photocatalytic degradation of the insecticide imidacloprid in aqueous solutions, *Appl. Catal., B*, 86 (2009) 27–35.
- [2] Y. Wang, H. Zhao, M. Li, J. Fan, G. Zhao, Magnetic ordered mesoporous copper ferrite as a heterogeneous Fenton catalyst for the degradation of imidacloprid, *Appl. Catal., B*, 147 (2014) 534–545.
- [3] H. Guan, D. Chi, J. Yu, H. Li, Dynamics of residues from a novel nano-imidacloprid formulation in soyabean fields, *Crop Prot.*, 29 (2010) 942–946.
- [4] R. Žabar, T. Komel, J. Fabjan, M.B. Kralj, P. Trebše, Photocatalytic degradation with immobilised  $\text{TiO}_2$  of three selected neonicotinoid insecticides: imidacloprid, thiamethoxam and clothianidin, *Chemosphere*, 89 (2012) 293–301.
- [5] P. Jovanov, V. Guzsvány, S. Lazić, M. Franko, M. Sakač, L. Šarić, J. Kos, Development of HPLC-DAD method for determination of neonicotinoids in honey, *J. Food Compos. Anal.*, 40 (2015) 106–113.
- [6] S. Malato, J. Caceres, A. Aguera, M. Mezcua, D. Hernando, J. Vial, A.R. Fernandez-Alba, Degradation of imidacloprid in water by photo-Fenton and  $\text{TiO}_2$  photocatalysis at a solar pilot plant: a comparative study, *Environ. Sci. Technol.*, 35 (2001) 4359–4366.
- [7] M.A. Radwan, M.S. Mohamed, Imidacloprid induced alterations in enzyme activities and energy reserves of the land snail, *Helix aspersa*, *Ecotoxicol. Environ. Saf.*, 95 (2013) 91–97.
- [8] S. Baskaran, R.S. Kookana, R. Naidu, Determination of the insecticide imidacloprid in water and soil using high-performance liquid chromatography, *J. Chromatogr., A*, 787 (1997) 271–275.
- [9] M. Rani, U. Shanker, V. Jassal, Recent strategies for removal and degradation of persistent and toxic organochlorine pesticides using nanoparticles: a review, *J. Environ. Manage.*, 190 (2017) 208–222.
- [10] W.J. Liu, T.T. Qian, H. Jiang, Bimetallic Fe nanoparticles: recent advances in synthesis and application in catalytic elimination of environmental pollutants, *Chem. Eng. J.*, 236 (2014) 448–463.

- [11] H.K. Boparai, M. Joseph, D.M. O'Carroll, Kinetics and thermodynamics of cadmium ion removal by adsorption onto nano zero valent iron particles, *J. Hazard. Mater.*, 186 (2011) 458–465.
- [12] M. Vitkov, M. Puschenreiter, M. Komarek, Effect of nano zero-valent iron application on As, Cd, Pb, and Zn availability in the rhizosphere of metal(loid) contaminated soils, *Chemosphere*, 200 (2018) 217–226.
- [13] S. Li, W. Wang, F. Liang, W.X. Zhang, Heavy metal removal using nanoscale zero-valent iron (nZVI): theory and application, *J. Hazard. Mater.*, 322 (2017) 163–171.
- [14] Y.S. El-Temseh, A. Sevcu, K. Bobcikova, M. Cernik, E.J. Joner, DDT degradation efficiency and ecotoxicological effects of two types of nano-sized zero-valent iron (nZVI) in water and soil, *Chemosphere*, 144 (2016) 2221–2228.
- [15] Y.S. Keum, Q.X. Li, Reduction of nitroaromatic pesticides with zero valent iron, *Chemosphere*, 54 (2004) 255–263.
- [16] S. Roman, M.L. Alonso, L. Bartolome, A. Galdames, E. Goiti, M. Ocejo, M. Moraques, R.M. Alonso, J.L. Vilas, Relevance study of bare and coated zero valent iron nanoparticles for lindane degradation from its by-product monitirization, *Chemosphere*, 93 (2013) 1324–1332.
- [17] Z.X. Chen, X.Y. Jin, Z. Chen, M. Megharaj, R. Naidu, Removal of methyl orange from aqueous solution using bentonite-supported nanoscale zero-valent iron, *J. Colloid Interface Sci.*, 363 (2011) 601–607.
- [18] J. Fan, Y. Guo, J. Wang, M. Fan, Rapid decolorization of azo dye methyl orange in aqueous solution by nanoscale zerovalent iron particles, *J. Hazard. Mater.*, 166 (2009) 904–910.
- [19] J. Lin, M. Sun, X. Liu, Z. Chen, Functional kaolin supported nanoscale zero-valent iron as a Fenton-like catalyst for the degradation of Direct Black G, *Chemosphere*, 184 (2017) 664–672.
- [20] Y. Liu, S. Zha, D. Rajarathnam, Z. Chen, Divalent cations impacting on Fenton-like oxidation of amoxicillin using nZVI as a heterogeneous catalyst, *Sep. Purif. Technol.*, 188 (2017) 548–552.
- [21] W. Zhang, H. Gao, J. He, P. Yang, D. Wang, T. Ma, H. Xia, X. Xu, Removal of norfloxacin using coupled synthesized nanoscale zero-valent iron (nZVI) with H<sub>2</sub>O<sub>2</sub> system: optimization of operating conditions and degradation pathway, *Sep. Purif. Technol.*, 172 (2017) 158–167.
- [22] Y. Li, F. Fu, Z. Ding, Removal of nitrate from water by acid-washed zero-valent iron/ferrous ion/hydrogen peroxide: influencing factors and reaction mechanism, *Water Sci. Technol.*, 77 (2018) 525–533.
- [23] Q. Wu, C. Zheng, J. Zhang, F. Zhang, Nitrate removal by a permeable reactive barrier of Fe<sup>0</sup>: a model based evaluation, *J. Earth Sci.*, 28 (2017) 447–456.
- [24] H. Dong, Q. He, G. Zeng, L. Tang, L. Zhang, Y. Xie, Y. Zeng, F. Zhao, Degradation of trichloroethene by nanoscale zero-valent iron (nZVI) and nZVI activated persulfate in the absence and presence of EDTA, *Chem. Eng. J.*, 316 (2017) 410–418.
- [25] I. Dror, O.M. Jacov, A. Cortis, B. Berkowitz, Catalytic transformation of persistent contaminants using a new composite material based on nanosized zero valent iron, *ACS Appl. Mater. Interfaces*, 4 (2012) 3416–3423.
- [26] N. Krasae, K. Wantala, Enhanced nitrogen selectivity for nitrate reduction on Cu-nZVI by TiO<sub>2</sub> photocatalysts under UV irradiation, *Appl. Surf. Sci.*, 380 (2016) 309–317.
- [27] K. Pawlak, J. Fronczyk, K. Garbulewski, Reactivity of nano zero valent iron in permeable reactive barriers, *Pol. J. Chem. Technol.*, 17 (2015) 1–7.
- [28] M. Turabik, U.B. Simsek, Effect of synthesis parameters on the particle size of the zero valent iron nanoparticles, *Inorg. Nano Metal Chem.*, 47 (2017) 1033–1043.
- [29] S. Xavier, R. Gandhimathi, P.V. Nidheesh, S. Thanga Ramesh, Comparative removal of Magenta MB from aqueous solution by homogeneous and heterogeneous photo-Fenton processes, *Desal. Wat. Treat.*, 57 (2015) 12832–12841.
- [30] H. Tamura, K. Goto, T. Yotsuyanagi, M. Nagayama, Spectrophotometric determination of Iron (II) with lio-phenanthroline in the presence of large amounts of Iron (III), *Talanta*, 21 (1973) 314–318.
- [31] P.V. Nidheesh, R. Gandhimathi, S. Velmathib, N.S. Sanjini, Magnetite as a heterogeneous electro Fenton catalyst for the removal of Rhodamine B from aqueous solutions, *RSC Adv.*, 4 (2014) 5698.
- [32] A. Liu, J. Liu, B. Pan, W. Zhang, Formation of lepidocrocite (g-FeOOH) from oxidation of nanoscale zero-valent iron (nZVI) in oxygenated water, *RSC Adv.*, 4 (2014) 57377.
- [33] C.B. Wang, W.X. Zhang, Synthesizing nanoscale iron particles for rapid and complete dechlorination of TCE and PCBs, *Environ. Sci. Technol.*, 31 (1997) 2154–2156.
- [34] F. Fua, D.D. Dionysiou, H. Li, The use of zero valent iron for groundwater remediation and wastewater treatment: a review, *J. Hazard. Mater.*, 267 (2014), 194–205.
- [35] S.H. Joo, A.J. Feitz, D.L. Sedlak, T.D. Waite, Quantification of the oxidizing capacity of nanoparticulate zero valent iron, *Environ. Sci. Technol.*, 39 (2005) 1263–1268.
- [36] C.R. Marcelo, R.P. Lopes, J.C. Cruz, M.A. Nascimento, A.A. Silva, C.F. Lima, Evaluation of different parameters on the acetamidrid degradation by bimetallic Fe/Ni nanoparticles, *Sep. Purif. Technol.*, 171 (2016) 256–262.
- [37] Y.H. Shih, C.P. Tso, L.Y. Tung, Rapid degradation of methyl orange with nanoscale zerovalent iron particles, *J. Environ. Eng. Manage.*, 20 (2010) 137–143.
- [38] M. Zhang, Q. Zhao, Z. Ye, Organic pollutants removal from 2,4,6-trinitrotoluene(TNT) red water using low cost activated coke, *J. Environ. Sci.*, 23 (2011) 1962–1969.
- [39] D.W. Elliott, H.L. Lien, W.X. Zhang, Degradation of lindane by zero valent iron nanoparticles, *J. Environ. Eng.*, 135 (2009) 317–324.
- [40] R. Rakhshae, Rule of Fe<sup>0</sup> nano-particles and biopolymer structures in kinds of the connected pairs to remove Acid Yellow 17 from aqueous solution: simultaneous removal of dye in two paths and by four mechanisms, *J. Hazard. Mater.*, 197 (2011) 144–152.
- [41] B.A. Lenell, Y. Arai, Perrhenate sorption kinetics in zerovalent iron in high pH and nitrate media, *J. Hazard. Mater.*, 321 (2017) 335–343.
- [42] A.J. Feitz, S.H. Joo, J. Guan, Q. Sun, D.L. Sedlak, T.D. Waite, Oxidative transformation of contaminants using colloidal zero valent iron, *Colloids Surf., A*, 265 (2005) 88–94.
- [43] X. Jin, Z. Chen, Z. Chen, R. Zhou, Synthesis of kaolin supported nanoscale zero-valent iron and its degradation mechanism of Direct Fast Black G in aqueous solution, *Mater. Res. Bull.*, 61 (2015) 433–438.
- [44] Y. Lin, Z. Chen, Z. Chen, M. Megharaj, R. Naidu, Decoloration of acid violet red B by bentonite-supported nanoscale zero-valent iron: reactivity, characterization, kinetics and reaction pathway, *Appl. Clay Sci.*, 93–94 (2014) 56–61.
- [45] J. Cao, L. Wei, Q. Huang, L. Wang, S. Han, Reducing degradation of azo dye by zero valent iron in aqueous solution, *Chemosphere*, 38 (1999) 565–571.
- [46] P.N. Moza, K. Hustert, E. Feicht, A. Kettrup, Photolysis of imidacloprid in aqueous solution, *Chemosphere*, 36 (1998) 497–502.
- [47] M.L. Dell'arciprete, J.L. Santos, A.A. Sanz, R. Vicente, A.M. Amat, J.P. Furlong, D.O. Martiere, M.C. Gonzalez, Reactivity of hydroxyl radicals with neonicotinoid insecticides: mechanism and changes in toxicity, *Photochem. Photobiol. Sci.*, 8 (2009) 1016–1023.
- [48] N. Schippers, W. Schwack, Photochemistry of imidacloprid in model systems, *J. Agric. Food Chem.*, 56 (2008) 8023–8029.
- [49] F. Bourgin, L. Violleau, J. Debrauwer, Ozonation of imidacloprid in aqueous solutions: reaction monitoring and identification of degradation products, *J. Hazard. Mater.*, 190 (2011) 60–68.
- [50] C. Noubactep, An analysis of the evolution of reactive species in Fe<sup>0</sup>/H<sub>2</sub>O systems, *J. Hazard. Mater.*, 168 (2009) 1626–1631.
- [51] S.H. Joo, D. Zhao, Destruction of lindane and atrazine using stabilized iron nanoparticles under aerobic and anaerobic conditions: effects of catalyst and stabilizer, *Chemosphere*, 70 (2008) 418–425.
- [52] J. Lin, X. Weng, R. Dharmarajan, Z. Chen, Characterization and reactivity of iron based nanoparticles synthesized by tea extracts under various atmospheres, *Chemosphere*, 169 (2017) 413–417.

- [53] A.W. McPherson, M.N. Goltz, A. Agrawal, *Pollutant Degradation by Nanoscale Zero Valent Iron (nZVI): Role of Polyelectrolyte Stabilization and Catalytic Modification on nZVI Performance*, American Chem. Soc. Dayton, Ohio, 2013, pp. 160–191.
- [54] A. Liu, J. Liu, J. Han, W. Zhang, Evolution of nanoscale zero-valent iron (nZVI) in water: microscopic and spectroscopic evidence on the formation of nano- and micro-structured iron oxides, *J. Hazard. Mater.*, 322 (2017) 129–135.
- [55] Y. Furukawa, J.W. Kim, J. Watkins, R.T. Wilkin, Formation of ferrihydrite and associated iron corrosion products in permeable reactive barriers of zero-valent iron, *Environ. Sci. Technol.*, 36 (2002) 5469–5475.
- [56] C. Noubactep, A critical review on the process of contaminant removal in  $\text{Fe}^0\text{-H}_2\text{O}$  systems, *Environ. Technol.*, 29 (2009) 909–920.
- [57] T.B. Scott, I.C. Popescu, R.A. Crane, C. Noubactep, Nano-scale metallic iron for the treatment of solutions containing multiple inorganic contaminants, *J. Hazard. Mater.*, 186 (2011) 280–287.
- [58] Y. Wu, J. Zhang, Y. Tong, X. Xu, Chromium (VI) reduction in aqueous solutions by  $\text{Fe}_3\text{O}_4$  stabilized  $\text{Fe}^0$  nanoparticles, *J. Hazard. Mater.*, 172 (2009) 1640–1645.
- [59] D. Redlich, N. Shahin, P. Ekici, A. Friess, H. Parlar, Kinetic study of the photoinduced degradation of imidacloprid in aquatic media, *Clean Soil Air Water*, 35 (2007) 452–458.
- [60] X. Liu, Y. Tian, X. Zhou, Z. Liu, L. Huang, Zero-valent aluminum as reducer in sodium carbonate solution for degradation of imidacloprid, *J. Chin. Chem. Soc.*, 63 (2016) 4754–4760.
- [61] J. Tang, X. Huang, X. Huang, L. Xiang, Q. Wang, Photocatalytic degradation of imidacloprid in aqueous suspension of  $\text{TiO}_2$  supported on H-ZSM-5, *Environ. Earth Sci.*, 66 (2012) 441–445.
- [62] M. Turabik, N. Oturan, B. Gozmen, M.A. Oturan, Efficient removal of insecticide imidacloprid from water by electrochemical advanced oxidation processes, *Environ. Sci. Pollut. Res. Int.*, 21 (2014) 8387–8397.